Clin. Vision Sci. Vol. 7, No. 6, pp. 521–530, 1992
Printed in Great Britain.

0887-6169/92 $5.00 + 0.00

THE EFFECT OF EYE SHAPE ON RETINAL RESPONSES

JU-FUN CHEN,[1,2]* ANN E. ELSNER,[1,3] STEPHEN A. BURNS,[1,3] RONALD M. HANSEN,[1,2]
PETER L. LOU,[1,4] KENNETH K. KWONG[1,5] and ANNE B. FULTON[1,2]†

[1]Department of Ophthalmology, Harvard Medical School, [2]Children's Hospital, [3]The Eye Research Institute, [4]Massachusetts Eye and Ear Infirmary and [5]NMR Center, Department of Radiology, Massachusetts General Hospital, Boston, Mass., U.S.A.

(Received 30 January 1992; in revised form 30 March 1992)

Summary—1. We investigated the size and shape of myopic eyes, and emmetropic and hyperopic control eyes, using refraction, ultrasonography, magnetic resonance imaging and scanning laser ophthalmoscope (SLO) imaging.

2. We measured full-field, scotopic sensitivities and saturated amplitudes of *b*-wave responses from these eyes.

3. The subjects' photopic psychophysical thresholds were measured at the posterior pole.

4. We find that saturated response amplitudes, but not sensitivities, are low in myopic subjects.

5. The psychophysical sensitivities are largely unaffected.

6. Eye shape is a better predictor of saturated response amplitude than eye size.

7. These results can be explained by low retinal cell responsivity, but not by increased spacing of retinal cells that would cause low sensitivity.

Key words—Myopia; hyperopia; a-scan ultrasonography; magnetic resonance imaging; electroretinogram; scanning laser ophthalmoscope.

INTRODUCTION

Eyes with high myopia often have scotopic and photopic *a*- and *b*-wave ERG responses that are smaller than normal (Blach *et al.*, 1966; Karpe, 1945; Pallin, 1969; Perlman *et al.*, 1984). The degree of response attenuation is inversely related to axial length (Pallin, 1969; Perlman *et al.*, 1984). Therefore, ERG attenuation has seemed attributable to the greater myopic eye size with enlarged posterior segment and retinal surface area. A mechanistic explanation of the small responses which considers retinal cells has, however, been wanting.

If all eyes are assumed to have about the same number of photoreceptors, then the enlarged myopic eye would have fewer receptors per unit area and more space between receptors than emmetropic or hyperopic eyes. This stretched retina hypothesis predicts less light per photoreceptor, and, therefore, greater stimulus intensity would be needed below response saturation to evoke the same size ERG response from a myopic as non-myopic eye. In other words, the stimulus intensity producing an unsaturated response of specified magnitude (the definition of sensitivity) would vary. However, this hypothesis does not predict attenuation of the saturated response amplitude. ERG response amplitude increases with flash intensity until amplitude saturates (Fig. 1), that is, until further increases in intensity cause no further growth in response amplitude (Fulton and Rushton, 1978). Therefore, effects on saturated response amplitude can be independent of variations in sensitivity.

As an alternative to the stretched retina hypothesis [Fig. 1(A)], in which spacing but not function of retinal elements varies, depressed retinal cell responsivity could explain attenuated ERG responses. According to this theory, saturated responses would be small but sensitivity, defined as the semisaturation constant, would be unaffected [Fig. 1(B)]. Previous ERG studies of myopia have not examined semisaturation constant and saturated response amplitude.

Either hypothesis is a plausible explanation of attenuated ERG responses of myopic eyes. Myopic fundi frequently have peripapillary crescents, posterior staphylomas, tessellated coloration and areas of retinal thinning that are

*On leave from the Department of Ophthalmology, Taipei Veterans General Hospital, Taipei, Taiwan.
†To whom all correspondence should be addressed at Department of Ophthalmology, Children's Hospital, 300 Longwood Avenue, Boston, MA 02115, U.S.A.

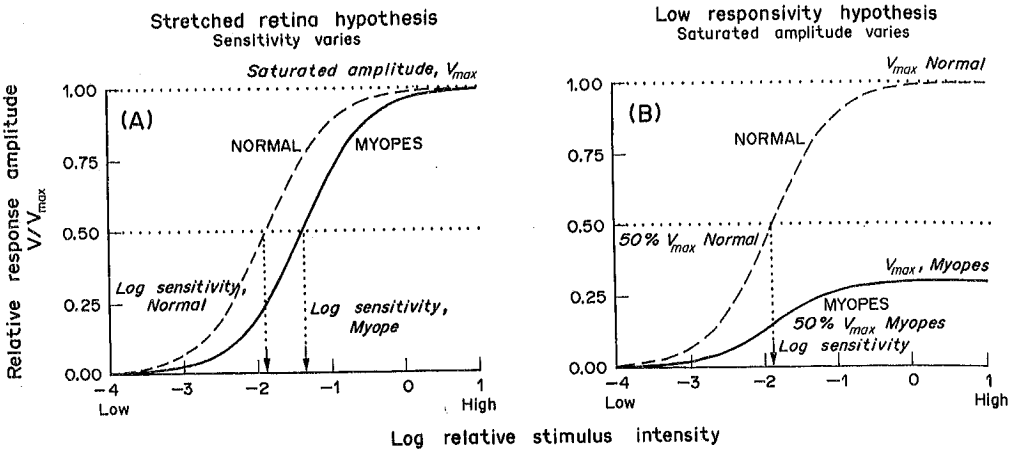

Fig. 1. Predictions of the stretched retina and low cell responsivity hypotheses. The curves plot equation (1) with the exponent n, set at unity and the stimulus I, on a log scale. In both panels the hypothetical stimulus–response relations for myopes are shown by the solid curves, and the normal stimulus–response relation is shown by the dashed curves. (A) The stretched retina hypothesis predicts variation of sensitivity but not of saturated response amplitude. (B) The low responsivity hypothesis predicts low saturated response amplitudes, but no variation in sensitivity, the intensity of stimulus required to produce a below saturation response of specified magnitude, for instance, 50% of the saturated amplitude as shown here.

ordinarily interpreted as indicative of a stretched, neural retina and thin pigment epithelium (e.g. Curtin, 1977). Staphylomata might be associated with secondary damage to retinal cells. However, myopic eyes can be selected to have good acuity and absence of staphylomata and ophthalmoscopic signs of degeneration to minimize the likelihood of decreased cell responsivity.

To test the stretched retina and reduced responsivity hypotheses, we use full-field electroretinographic procedures to evaluate (Fig. 1) amplitude of saturated responses and scotopic sensitivity (log σ). Across the posterior pole photopic sensitivities are measured psychophysically. In addition to axial length, measured along the visual axis by ultrasonography, imaging techniques characterize posterior segment size and shape.

MATERIALS AND METHODS

Subjects

Fifteen healthy subjects, ages 15–38 (median, 23.4) yr, participated (Table 1). Five were myopes (spherical equivalent −7.37 to −9.5 D), four were emmetropes (−0.5 to +0.25 D) and six were hyperopes (+4.25 to +7.75 D). Each eye of all su
corrected Snellen acuities of
well as good foveal reflexes.
M4 had slender peripapilla
cents, and all myopes had
posterior pole. However, n
rolled who had an ophthalmo
able posterior staphyloma or
peripheral chorioretinal dege
nature, purpose and risks
measurements were explain
sent was obtained from eac
from the parents of the 15 y

Keratometry, cycloplegic
ultrasonography, magnetic
(MRI), electroretinography
terior pole imaging and
threshold measurements wit
ophthalmoscope (SLO) were
one eye of each subject
all measurements were mad
(Tables 1 and 2). For exampl
was done only on the myop

Refraction and keratometry

After cyclopentolate 1% c
the subject was positioned at
fractor. Ten readings were
median determined (Table 1)

Table 1. Refraction, kerotometry and axial length of subjects

Subject	Age (yr)	Refraction (D)	Spherical equivalent (D)	Keratometry (D) vertical/horizontal	Axial length* (mm)
Myopes					
M1	19	−9.5	−9.5	44.5/43.6	26.2
M2	23	−8.0–1.62 × 90	−8.8	46.9/46.6	25.3
M3	31	−9.5	−9.5	46.7/45.9	25.6
M4	32	−7.0–0.75 × 90	−7.37	41.9/42.4	27.4
M5	18	−7.12–0.62 × 10	−7.43	45.0/45.5	24.6
Emmetropes					
E1	24	+0.25	+0.25	45.0/44.9	—
E2	27	−0.25	−0.25	45.2/44.9	—
E3	38	+0.25	+0.25	42.5/41.5	—
E4	38	−0.5	−0.5	42.7/43.1	—
Hyperopes					
H1	18	+4.25	+4.25	—	22.2
H2	15	+7.0–0.75 × 90	+6.63	—	21.5
H3	18	+8.0–0.5 × 70	+7.75	41.0/42.2	21.1
H4	22	+5.0	+5.0	—	—
H5	19	+5.37–0.75 × 40	+5.0	—	21.9
H6	24	+5.0–1.0 × 180	+4.5	42.2/44.0	22.0

*Spherical equivalent and axial length are correlated ($r = -0.94$, d.f. = 8, $P < 0.001$).

Subject	V_{max} (μV)	Scotopic F Log σ (log scot td s)
Myopia		
M1	327	−1.05
M2	469	−0.92
M3	253	−0.9
M4	339	−0.4
M5	301	−0.9
Emmetropia		
E1	452	−1.0
E2	—	—
E3	—	—
E4	256	−0.6
Hyperopia		
H1	436	−1.12
H2	520	−0.71
H3	433	−1.5
H4	477	−0.6
H5	696	−0.4
H6	382	−0.82

*The mean(± SD) b-wave paramet
log scot td s; n, 0.88(0.23).
†Amplitude of b-wave normal resp
‡Parameters from analysis of MRI.
(r.m.s., posterior segment)/(radi
§MRI of subject M2 was taken at
the r.m.s. errors and shape fac

+7.75 D). Each eye of all subjects studied had corrected Snellen acuities of 20/25 or better as well as good foveal reflexes. Myopes M1 and M4 had slender peripapillary temporal crescents, and all myopes had tessellation of the posterior pole. However, no myope was enrolled who had an ophthalmoscopically identifiable posterior staphyloma or signs of central or peripheral chorioretinal degeneration. After the nature, purpose and risks of the proposed measurements were explained, informed consent was obtained from each participant and from the parents of the 15 yr-old subject.

Keratometry, cycloplegic refraction, a-scan ultrasonography, magnetic resonance imaging (MRI), electroretinography (ERG), and posterior pole imaging and cone increment threshold measurements with a scanning laser ophthalmoscope (SLO) were performed. Only one eye of each subject was studied. Not all measurements were made on all subjects (Tables 1 and 2). For example, ultrasonography was done only on the myopes and hyperopes.

Refraction and keratometry

After cyclopentolate 1% or tropicamide 1%, the subject was positioned at the Canon autorefractor. Ten readings were obtained, and the median determined (Table 1). Keratometry was accomplished using a Bausch and Lomb keratometer. The cornea was positioned so that the zone of the optical axis coincided wih the axis of the instrument and the curvature of the apical zone of the cornea was measured. The median of three readings was recorded (Table 1).

Ultrasonography

The axial length along the visual axis was measured using the a-scan mode of the Cooper Vision Ultrascan-II instrument. During recording, the seated subject viewed a fixation light in the probe of the instrument. Four measurements were made when maximal amplitude spikes were obtained. The mean of these measurements along the visual axis was reported (Table 1).

Magnetic resonance imaging (MRI)

A General Electric Signa system (H0 = 1.5 T) with a 1-in. diameter surface coil and the spin–echo sequence (TR = 400–500 ms, TE = 20 ms) was used to obtain MR images. Both coronal and axial sections were obtained at 3 mm intervals across the extent of the globe. Negatives of these images were provided. On these negatives, the largest, most central axial section of each eye was selected for digitization. Using an IBM compatible computer imaging

Table 2. Results of ERG, SLO and MRI studies

	Scotopic ERG*				Photopic ERG†	SLO	MRI‡			
Subject	V_{max} (μV)	Log σ (log scot td s)	n	r.m.s.	b-amplitude (μV)	Fovea to disc (deg)	r.m.s. posterior segment	Radius posterior segment	Shape factor	r.m.s. posterior pole
Myopia										
M1	327	−1.05	0.6	0.048	54	15.6	1.018	12.3	0.083	0.745
M2	469	−0.92	0.8	0.032	109	11.38	0.235	10.8§	0.022	0.307
M3	253	−0.9	1.2	0.04	43	12.4	0.933	12.4	0.075	0.629
M4	339	−0.4	0.8	0.048	76	15.89	1.067	13.42	0.080	0.898
M5	301	−0.9	1.3	0.055	87	—	—	—	—	—
Emmetropia										
E1	452	−1.0	0.9	0.028	—	12.77	0.558	11.55	0.048	0.511
E2	—	—	—	—	—	12.7	0.272	11.27	0.024	0.181
E3	—	—	—	—	—	13.1	0.609	12.63	0.048	0.543
E4	256	−0.6	0.7	0.037	—	13.08	0.575	12.11	0.048	0.446
Hyperopia										
H1	436	−1.12	1.0	0.0418	108	13.1	0.333	10.89	0.031	0.185
H2	520	−0.71	0.7	0.053	103	—	—	—	—	—
H3	433	−1.5	1.1	0.041	179	—	—	—	—	—
H4	477	−0.6	1.0	0.066	212	—	—	—	—	—
H5	696	−0.4	0.6	0.045	152	11.49	0.227	11.14	0.020	0.14
H6	382	−0.82	1.1	0.037	136	12.88	0.406	11.47	0.035	0.38

*The mean(± SD) b-wave parameters (see text) for 27 emmetropic young adults are: V_{max}, 396(86) μV; log σ, −0.71(0.219) log scot td s; n, 0.88(0.23).

†Amplitude of b-wave normal response to 10 μs, red (Wratten 29), +0.9 log phot td s flashes: 79(8) μV.

‡Parameters from analysis of MRI. Radius of posterior segment: radius of the fitted circle; see text. Shape factor: the ratio (r.m.s., posterior segment)/(radius best fit circle); see text.

§MRI of subject M2 was taken at about 2 times magnification. Thus, the radii for M2 differ in absolute length. However, the r.m.s. errors and shape factor are comparable, across subjects.

system and video camera, at least 40 points about equally spaced along the perimeter of the posterior segment of each eye were digitized. All points were at the inner margin of choroid; the retina could not be identified on these images. Then, using a Simplex minimization routine (Caceci and Cacheris, 1984) a circle was fitted to the digitized posterior segment using a minimum r.m.s. error criterion.

The fovea was not visible on the MR images (Fig. 2). The following procedure was used to find the foveal site on the MR images. On SLO images, the pixels between the fovea and the temporal disc margin were counted. Next, the angle between the fovea and temporal disc margin, measured on each subject's SLO image, was calculated in degrees of visual angle. Then the disc margin was identified on the MR images. The visual angle was transformed to the angular position on the MR images. A polar coordinate system was then defined with the origin at the center of the fitted circle, the fovea at 180°, the temporal equator toward 90° and nasal equator toward 270°.

The ratio between the distance measured from the center of the fitted circle to the digitized point on the choroidal margin, and the radius of the circle provided a measure of the deviation from a circle at every point. Thus, for a point on the circle, the ratio was 1. For points outside the circle, the ratio is >1. The more the ratio deviated from 1, the greater the eye deviated from circularity.

The ratio of the r.m.s. error of the entire posterior segment and the radius of the best fit circle was used as an index of the overall shape of the posterior segment. This ratio was defined as the shape factor.

Besides the r.m.s. error for the entire posterior segment, the r.m.s. error of the posterior pole was determined. The posterior pole was defined as 10° nasal and temporal from the fovea, that is, the segment from 170 to 190°.

ERG

The subject, with dilated pupil, adapted in the dark for 30 min. Then, after instillation of proparacaine 0.5%, a Burian–Allen type bipolar electrode was placed on the eye. The ground electrode was placed on the skin over the ipsilateral mastoid. Flashed (Grass PS22; 10 μs), blue (Wratten 47B; $\lambda < 510$ nm) stimuli were presented via a 16 in. integrating sphere. A scotopic stimulus–response function was obtained by starting with a dim flash that produced a small *b*-wave visible on a single sweep. The interstimulus interval was chosen so that successive flashes did not attenuate the *b*-wave; it ranged from 2 s for dim flashes to 10 s for the brightest flashes. Flash intensity was increased to maximum intensity in 0.3 log unit steps. At full intensity, the blue stimulus produced a retinal illumination of +1.2 log scot td s.

Photopic responses to a red (Wratten 29; $\lambda > 610$ nm) flash producing about +0.9 log phot td s were also studied. The responses were recorded and amplified (a.c. coupled; gain = 1,000) using a Nicolet Compact 4 system and bandwidth 1–1000 Hz. 4–16 responses were averaged in each stimulus condition. A voltage window was used to reject large changes in potentials such as those caused by blinks. The records were stored to disk for later analysis.

The trough-to-peak *b*-wave amplitudes were measured. The *b*-wave stimulus–response data obtained with blue flashes were fitted by the equation

$$V/V_{max} = (I^n)/(I^n + \sigma^n) \quad (1)$$

where V was the *b*-wave amplitude produced by a flash of intensity I, and σ, the value of I that produced half of V_{max}, the saturated *b*-wave amplitude (Fulton and Rushton, 1978). Sensitivity was indexed by log σ. An iterative computer algorithm was used to find the values of V_{max}, σ, and n that minimize the r.m.s. deviation from the equation. ERG results were compared to those previously obtained by us from normal young adults.

Scanning laser ophthalmoscope

Using previously described procedures, we measured increment thresholds along the horizontal meridian while imaging the fundus with dim, 830 nm light (Elsner *et al.*, 1992). Test targets were 21 or 3.5 min arc diameter squares, 633 nm, 200 ms duration flashes presented on a steady, 1.7 log phot td, 633 nm background. The 21 min arc test was presented on a 28.6 × 23° field to test 0–17° nasal and temporal to the fovea. The 3.5 min arc target was presented on a 15.2 × 13.6° field to test 0–5° nasal and temporal to the fovea. Images of each eye with about half of the optic disc in view, combined with the computer graphics indicating fixation, were stored for comparison to MRI data.

Previous work showed thresholds near fixation had little variation with eccentricity (van de Velde *et al.*, 1991). Data were folded

Fig. 2. Positives of MR
emme

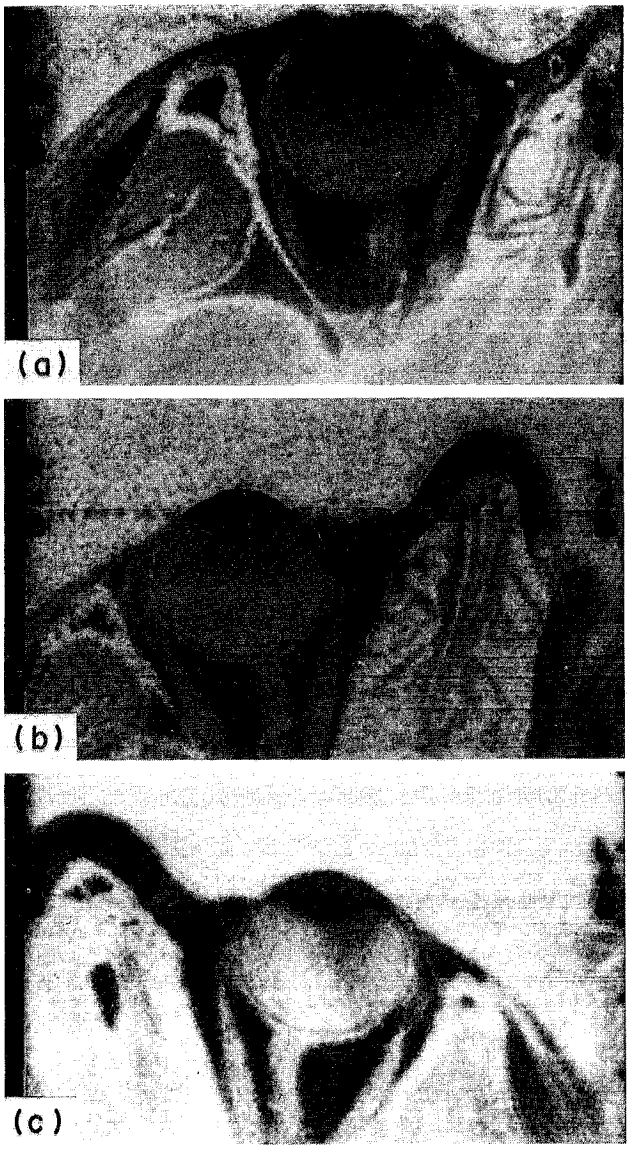

Fig. 2. Positives of MR images. These are unenlarged, axial views. The eyes of myopic subject M1 (a), emmetropic subject E1 (b) and hyperopic subject H6 (c) are shown.

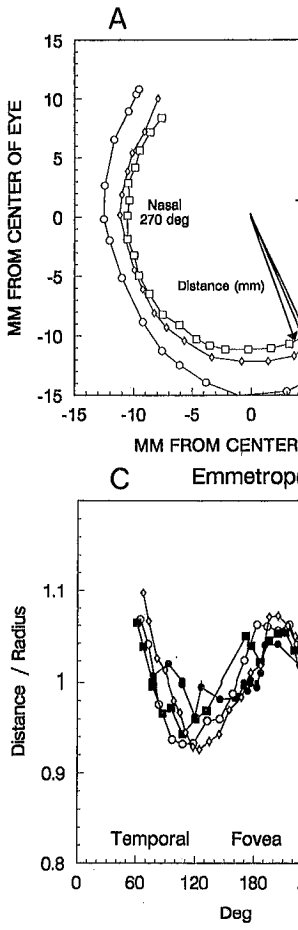

Fig. 3. The method for det
results. (A) Comparison o
curves are positioned so t
emmetropic and hyperopic
procedure, and each curve
each digitized point to the
long arrow indicates the po
270°. (B, C, D) Deviation
center of fitted circle to di
location of the digitized po
more from circularity that
round, but have less pron

about 0° and four values of
were calculated by linear r
subject. Two are central mea
target sizes, the third pe
(3.5 min arc data), and the f
2° (21 min arc data).

RESULTS

All axial lengths (Table
subjects are greater than tho
subjects. The spherical equ
lengths are correlated (Tabl
segment of the hyperopic s

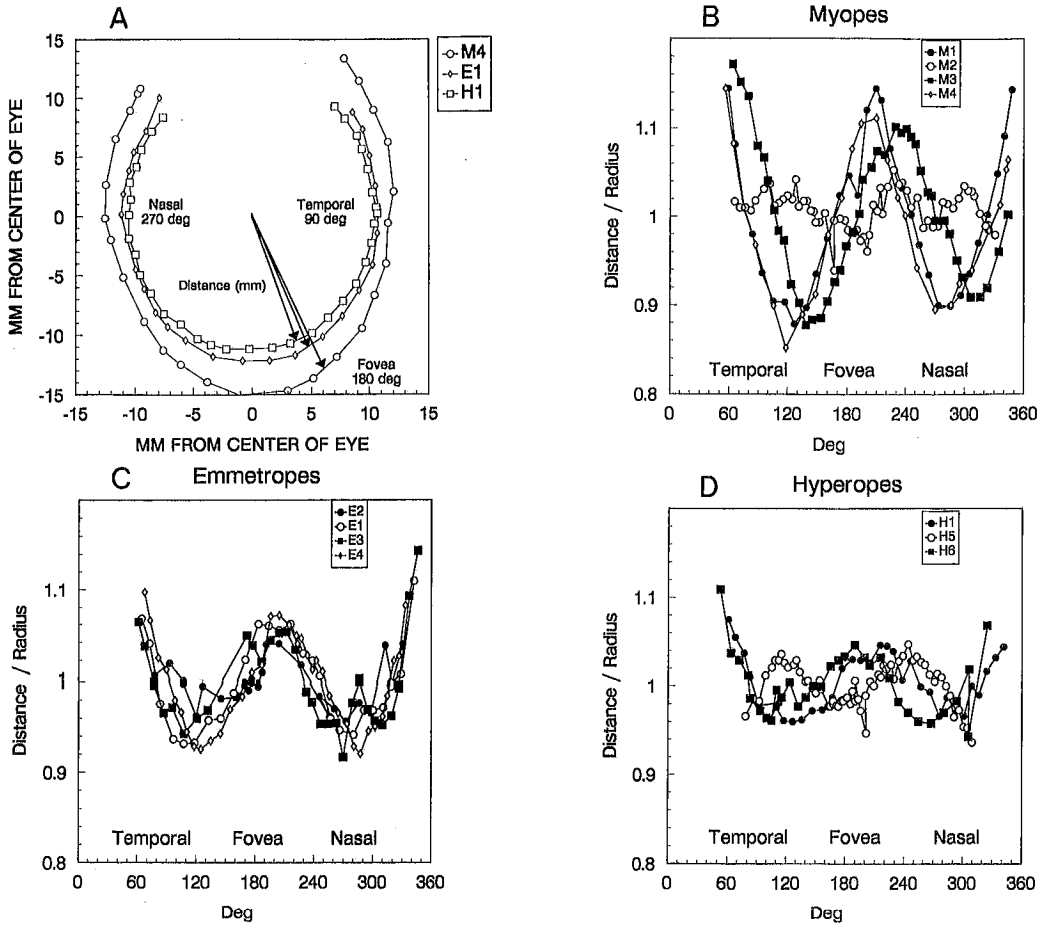

Fig. 3. The method for determining eyeball radius and shape, from digitized MRI pictures. Representative results. (A) Comparison of eyeball shape and size for myope M4, emmetrope E1 and hyperope H1. All curves are positioned so that the center of the cornea points up. The myopic eye is larger than the emmetropic and hyperopic eyes. The circle that best fits these points is calculated using a least squares procedure, and each curve is slid so that the center is plotted at the origin. Next, the angular relation of each digitized point to the optic nerve and fovea location on the subject's SLO image is determined. The long arrow indicates the position of the fovea, 180°. The temporal equator is toward 90°, the nasal toward 270°. (B, C, D) Deviation of posterior segment from fitted circle. In each panel the ratio: (distance from center of fitted circle to digitized point)/(the radius of the circle) is shown as a function of the angular location of the digitized point. The fovea is at 180°. Except for subject M2, the myopic eyes (B) deviated more from circularity that the emmetropic (C) or hyperopic (D) eyes. Emmetropic eyes are not perfectly round, but have less pronounced peaks and troughs than myopic eyes. Of the three refractive groups, hyperopic eyes are best fitted by the circle.

about 0° and four values of the Weber fraction were calculated by linear regression for each subject. Two are central measures using the two target sizes, the third peripheral to 0.75° (3.5 min arc data), and the fourth peripheral to 2° (21 min arc data).

RESULTS

All axial lengths (Table 1) of the myopic subjects are greater than those of the hyperopic subjects. The spherical equivalents and axial lengths are correlated (Table 1). The posterior segment of the hyperopic subjects are best fit by the circle, the myopic eyes most poorly fit (Table 2; Fig. 3). Among the myopic subjects, the posterior segment of subject M2 is exceptionally well fit by the circle. For the myopic eyes the greatest departure from circularity [Fig. 3(B)] is at the disc and temporal equator, the region that includes the approximate site of the posterior edge of the vitreous base where vitreous traction and horseshoe tears tend to occur (e.g. Karlin and Curtin, 1976; Tolentino *et al.*, 1972).

In the myopic eyes smaller departures from circularity are found at the posterior pole (here

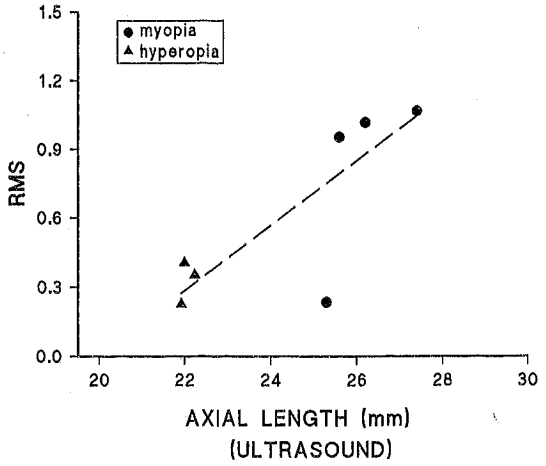

Fig. 4. Correlation between r.m.s. error of the posterior segment and axial length. The greater the r.m.s. error, the greater the deviation from circularity. The regression line has the equation $y = 0.134x - 2.67$.

defined as within 10° visual angle of the fovea) than in the region of the equator and disc. Indeed, with the exception of M2, the r.m.s. errors of the posterior pole are less than for the posterior segment as a whole. The ratio of the r.m.s. error of posterior pole and r.m.s. error of whole posterior segment is <1 in all myopic eyes except for subject M2, who had a very round eye [Fig. 3(B)]. Furthermore, the fovea to disc distance differs little among subjects. Nevertheless, across the fovea of all myopes the departure from circularity is quite large. This is in accord with the previously reported displaced directional sensitivity of the myopic fovea (Westheimer, 1968).

Eye shape, whether expressed as the r.m.s. error of the circle fit to the entire posterior segment (Fig. 4), the r.m.s. error of posterior pole, or the shape factor, is correlated with axial length [Table 3(A)]. Again, the myopic eyes, which have the greatest axial length, tend to have the greatest departure from circularity.

The scotopic *b*-wave intensity–response functions [Fig. 5(A)] of myopic and hyperopic subjects are equally well fit by equation (1); the r.m.s. errors of these functions (Table 2) do not differ significantly between myopes and hyperopes ($t = -0.452$; d.f. 9; $P > 0.05$). V_{max} for myopes is significantly smaller than for hyperopes ($t = -2.905$; d.f. $= 9$; $P < 0.2$). V_{max} is correlated with spherical equivalent [Fig. 5(B)]. V_{max} of each myopic subject except M2 is smaller than the normal mean, but all are within two standard deviations of the normal mean (Table 2, footnote). Sensitivity (log σ), does not differ between myopes and hyperopes. Of the variables spherical equivalent, axial length and shape factor, shape factor (Fig. 6) is the best predictor of V_{max} [Table 3(B)]. Stepwise addition of these variables, or other shape and size variables, does not improve the prediction.

Table 3. Pearson product moment correlations for subjects with ERG, MRI and ultrasonographic measures

(A) Eye shape parameters	vs	Axial length
r.m.s., posterior segment		0.87*
r.m.s., posterior pole		0.87†
Shape factor		0.78*
(B) Eye size and shape variables	**vs**	**V_{max}**
Spherical equivalent		0.59*
Axial length		−0.60*
Shape factor		−0.75*

*$P < 0.01$; †$P < 0.05$.

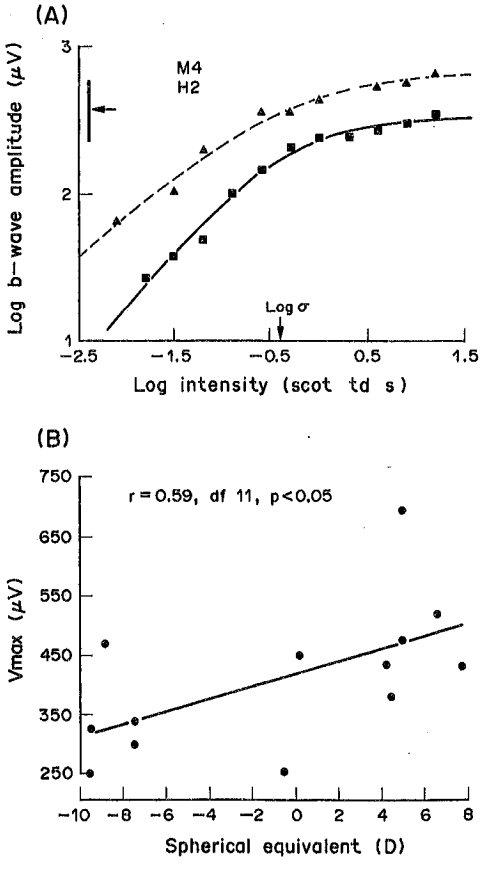

Fig. 5. Scotopic ERG responses. (A) Sample stimulus–response function from myopic subject M4 and hyperopic subject H2. The curves, representing equation (1), plotted on log–log coordinates, are fitted to the subjects' data. The *b*-wave amplitude (V_{max}) of the myope is lower than that of the hyperope, but retinal sensitivity (log σ), the stimulus producing a half-maximum response, does not differ. The large arrowhead and shaded bar indicate the normal mean ±2 SD values of log V_{max}. (B) Correlation between V_{max} and spherical equivalent. The regression line has the equation $y = 0.0105x + 0.4189$.

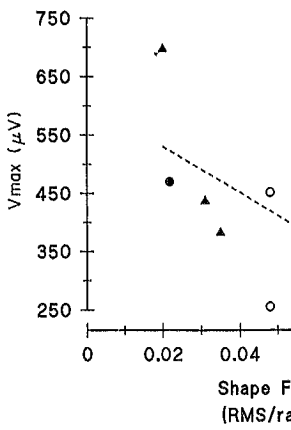

Fig. 6. V_{max} as a function of the s
ratio of the r.m.s. error of the wh
radius of the best fit circle. Th
equation $y = -4.5($

The amplitude of the
(Table 2) of myopes is signi
that of hyperopes (t =
$P < 0.01$). The photopic b-
spherical equivalent are
d.f. $= 9$; $P < 0.05$).

The Weber fractions are
opic ($n = 4$), emmetropic (
($n = 3$) subjects. Represe
shown in Fig. 7. Near fixat
fractions for the 3.5 min a
21 min arc targets, do no
between myopes and hype
the slopes of the Weber fr
steeper for the 3.5 min a
target. The Weber fraction
not differ significantly be
hyperopes. Thus, cone se
terior pole of these hypero
does not differ. None of
measures correlated with a
size parameters.

DISCUSSI

Despite the significant d
tween myopes and hypero
full-field scotopic sensitivi
Photopic psychophysical se
terior pole of myopes ar
b-wave amplitudes are si
myopes than hyperopes. T
consistent with decrease
[Fig. 1(B)], but offer little
pothesis that the myopic e
light per receptor and mo
receptors [Fig. 1(A)].

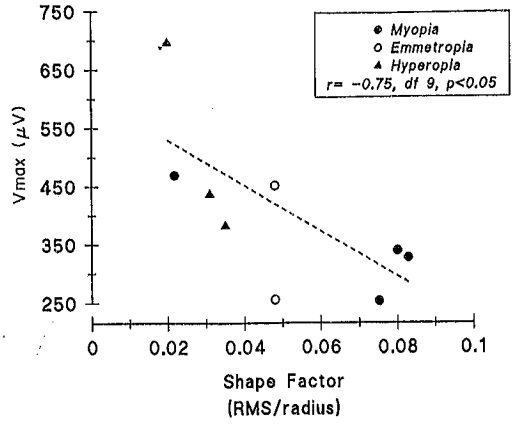

Fig. 6. V_{max} as a function of the shape factor, defined as the ratio of the r.m.s. error of the whole posterior segment and radius of the best fit circle. The regression line has the equation $y = -4.567x + 0.641$.

The amplitude of the photopic b-wave (Table 2) of myopes is significantly smaller than that of hyperopes ($t = -4.204$; d.f. $= 9$; $P < 0.01$). The photopic b-wave amplitude and spherical equivalent are correlated ($r = 0.77$; d.f. $= 9$; $P < 0.05$).

The Weber fractions are similar for the myopic ($n = 4$), emmetropic ($n = 4$) and hyperopic ($n = 3$) subjects. Representative results are shown in Fig. 7. Near fixation, the mean Weber fractions for the 3.5 min arc and also for the 21 min arc targets, do not differ significantly between myopes and hyperopes. Eccentrically, the slopes of the Weber fraction functions are steeper for the 3.5 min arc than 21 min arc target. The Weber fractions at 2° and at 10° do not differ significantly between myopes and hyperopes. Thus, cone sensitivity at the posterior pole of these hyperopic and myopic eyes does not differ. None of the Weber fraction measures correlated with any MRI shape and size parameters.

DISCUSSION

Despite the significant difference in V_{max} between myopes and hyperopes, no difference in full-field scotopic sensitivity (log σ) is found. Photopic psychophysical sensitivities at the posterior pole of myopes are normal. Photopic b-wave amplitudes are significantly lower in myopes than hyperopes. Thus, these data are consistent with decreased cell responsivity [Fig. 1(B)], but offer little support for the hypothesis that the myopic eye has less effective light per receptor and more light lost between receptors [Fig. 1(A)].

The shape of the posterior segment, rather than size and axial length alone, appears to be a critical determinant of V_{max}. For instance, subject M2, whose axial length (25.3 mm) is greater than that of any hyperope, has a V_{max} of 496 μV which is about the same as the median V_{max} for the hyperopic subjects (Table 2). In the entire sample only subject H5 has a smaller shape factor than M2. Furthermore, V_{max} is best predicted by shape factor, not axial length or spherical equivalent [Table 3(B)].

Assuming that there are about the same number of receptors in all eyes, the shape changes found in most myopic eyes (Fig. 3) would necessarily cause greater receptor to receptor cell spacing, and distort receptor to pigment epithelial cell relations. It has been suggested that these changes would increase the resistance (Pallin, 1969) in retinal tissue with consequent attenuation of response amplitude. However, this is exactly the opposite of what is predicted

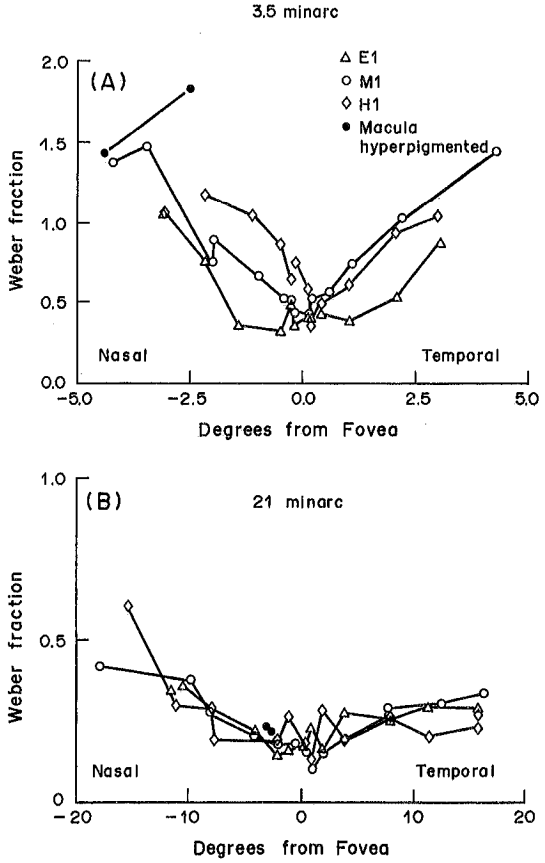

Fig. 7. Weber fractions of myopic, emmetropic and hyperopic subjects. Weber fractions of M1, E1 and H1. (A) Results of testing the central 5° with the 3.5 min arc target. Results of testing within 17° eccentricity using the 21 min arc target. In (A) and (B) the contrast needed to detect a target on a uniform background, the Weber fraction, is plotted as a function of eccentricity from the fovea (0°).

by Ohm's law, $V = IR$, and also contrary to ERG model predictions of voltages at the cornea (Rodieck, 1973). If the resistance model is used, then the present results require a decreased resistance.

It appears plausible that distortions of eye shape cause subtle disruptions of receptor-pigment epithelial-Bruch's membrane relations and consequent impairment of function of the pigment epithelial–receptor complex where ERG responses originate (e.g. Karowski, 1991). Evidence of localized, subclinical fundus abnormalities associated with impaired function are documented in subject M1. Compromised responsivity of cells, with the effect amplified by the *b*-wave generators, can account for the low, saturated responses from myopic eyes. In two other instances, infants and patients early in the course of retinal degeneration, low saturated *b*-wave response amplitudes are attributable to low retinal cell responsivity, caused by immaturity or disease, rather than low cell packing density (Fulton and Hansen, 1985, 1988; Hansen and Fulton, 1992).

In summary, these results suggest that low retinal cell responsivity, rather than mere enlargement of the eye with wider spacing of retinal elements, explains the low amplitude *b*-wave responses from myopic eyes. From a practical point of view, these results indicate V_{max} below a laboratory's fifth percentile cannot comfortably be ascribed to accompaning myopia of 7–10 D. Rather, additional diagnoses, such as those of retinal degenerations or functional anomalies, warrant consideration.

Acknowledgements—This work was supported by EY07624 (AEE, SAB), EY05329 (ABF, RMH), EY05325 (ABF, RMH) and the Massachusetts Lions Eye, EY07620 (HMC, KKK) Research Fund. Dr Chen was supported by a Taipei Veterans General Hospital fellowship. Dr Hong-Ming Cheng, Massachusetts Eye and Ear Infirmary, made the MRI coil available. Dr Robert H. Webb, the Eye Research Institute, Boston, provided critical comment, advice and the video system for analysis of the MRI pictures.

REFERENCES

Blach R. K., Jay B. and Kolb H. (1966) Electrical activity of the eye in high myopia. *Br. J. Ophthal.* **50,** 629–641.

Caceci M. S. and Cacheris W. P. (1984) Fitting curves to data. *Byte*, May.

Curtin B. J. (1977) The posterior staphyloma of pathologic myopia. *Trans. Am. ophthal. Soc.* **75,** 67–79.

Elsner A. E., Burns, Hughes and Webb (1992) Reflectometry with a scanning laser ophthalmoscope. *Appl. Opt.* (In press.)

Fulton A. B. and Hansen R. M. (1985) Electroretinography: application to clinical studies of infants. *J. Pediat. Ophthal. Strabis.* **22,** 251–255.

Fulton A. B. and Hansen R. M. (1988) Scotopic stimulus/response functions of the *b*-wave of the electroretinogram. *Documenta Ophthal.* **68,** 293–304.

Fulton A. B. and Rushton W. A. H. (1978) The human rod ERG: correlation with psychophysical response in light and dark adaptation. *Vision Res.* **18,** 793–800.

Hansen R. M. and Fulton A. B. (1992) The development of scotopic retinal sensitivity. In *Infant Vision: Basic and Clinical Research*, edited by Simons K. Oxford University Press, New York.

Karlin D. B. and Curtin B. J. (1976) Peripheral chorioretinal lesions and axial length of the myopic eye. *Am. J. Ophthal.* **8,** 625–635.

Karpe G. (1945) The basis of clinical electroretinopathy. *Acta ophthal.* **24** (Suppl.), 5–118.

Karwoski C. (1991) Introduction to the origins of electroretinographic components. *Principles and Practice of Clinical Electrophysiology of Vision*, edited by Heckenlively J. R. and Arden G. B., Chap. 8, pp. 87–90. Mosby, St Louis, Mo.

Pallin O. (1969) Influence of axial length of the eye on the size of the recorded *b*-potential in the clinical single-flash electroretinogram. *Acta ophthal.* **47** (Suppl.), 1–57.

Perlman I., Meyer E., Haim T. and Zonis S. (1984) Retinal function in high refractive error assessed electroretinographically. *Br. J. Ophthal.* **68,** 79–84.

Rodieck R. W. (1973) *The Vertebrate Retina*, pp. 534–536. W. H. Freeman, San Francisco, Calif.

Tolentino F. I., Schepens C. and Pomerantzeff O. (1972) Advances in the technique of vitreous cavity examination. In *Retina Congress*, edited by Pruett R. C. and Regan C. D. J., Chap. 16, pp. 215–227. Appleton Century Crofts, New York.

van de Velde F. J., Jalkh A. E. and Elsner (1991) Microperimetry with the scanning laser ophthalmoscope. In *Perimetry Update, 1990/1991*, edited by Mills R. P. and Heijl A., pp. 93–101. Kugler, Amsterdam.

Westheimer G. (1968) Entoptic visualization of Stiles–Crawford effect: an indicator of eyeball shape. *Archs ophthal.* **79,** 584–588.

Clin. Vision Sci. Vol. 7, No. 6, pp. 531
Printed in Great Britain

VALUE OF S
THE EVALU
PATIENTS W
WITH MACUI
OPHTHA
OI

JEAN-FRANÇ

[1]Service de Biophysique,
Ced

(R

Summary—1. The aim o
chart" presented convent
then by means of a mod
the optotype onto the ret
and a moderate lens op
2. The results obtaine
macular degeneration),
characters compared wit
3. The improvement
conventional conditions.
measured in part of the
obtained with the SLO
4. All of these results
opacities and demonstra
in patients with associat

Key words—Moderate c
acuity.

INTRODUC

Increasingly frequently, pa
moderate lens opacities c
gists with the desire to
compatible with the visual
ern life. Ophthalmologist
question of the indication
particularly difficult when
ate and allows a macular
on ocular fundus examina
this decision has been ba
clinical examination, in pa
of the visual acuity by
numbers presented on an
physiological investigation
(ERG) and visual evoke
(VECP)]. These investigati